The Journal of Experimental Biology 208, 1421-1433
Published by The Company of Biologists 2005
doi:10.1242/jeb.01552

Prey-capture in *Pomacanthus semicirculatus* (Teleostei, Pomacanthidae): functional implications of intramandibular joints in marine angelfishes

Nicolai Konow* and David R. Bellwood

Centre for Coral Reef Biodiversity, Department of Marine Biology, James Cook University, Townsville, Queensland 4811, Australia

*Author for correspondence (e-mail: nicolai.konow@jcu.edu.au)

Accepted 22 February 2005

Summary

We examined prey-capture morphology and kinematics in the angelfish, *Pomacanthus semicirculatus* (Cuvier 1931), to evaluate the magnitude and role of functional specialisation. The feeding apparatus of *P. semicirculatus* possess three biomechanical mechanisms of particular interest: (1) a novel intramandibular joint, permitting dentary rotation and protruded jaw closure; (2) an opercular linkage facilitating mandible depression; and (3) a suspensorial linkage with two novel points of flexion, permitting anterior rotation of the suspensorium and augmenting mandible protrusion. Prey-capture kinematics were quantified using motion analysis of high-speed video, yielding performance profiles illustrating timing of onset, duration and magnitude of movement in these three biomechanical systems, and other variables traditionally quantified in studies of teleostean ram–suction feeding activity. Mandible depression and suspensorial rotation both augmented mandible protrusion, and coincided during jaw protrusion, typically increasing head length by 30%. Jaw closure appeared to result from contraction of the adductor mandibulae segment A2, which rotated the dentary by approximately 30° relative to the articular. This resulted in jaw closure with the mandible fully depressed and the jaws at peak-protrusion. Feeding events were concluded by a high-velocity jaw retraction (20–50 ms), and completed in 450–750 ms. Feeding kinematics and morphology of *Pomacanthus* differed from other biting teleosts, and more closely resemble some long-jawed ram–suction feeders. The structural and functional modifications in the *Pomacanthus* feeding apparatus are matched to an unusual diet of structurally resilient and firmly attached benthic prey.

Supplementary material available online at
http://jeb.biologists.org/cgi/content/full/207/8/1421/DC1

Key words: feeding kinematics, biomechanics, functional morphology, mandible protrusion, suspensorial rotation, feeding mode, coral reef fish.

Introduction

Numerous studies have examined the associations between feeding apparatus functional morphology, biomechanics and prey-capture kinematics in teleost fishes (see reviews by Liem, 1980; Motta, 1984; Ferry-Graham and Lauder, 2001; Wainwright and Bellwood, 2002). These analyses have either tested or benefited directly from mathematical modelling of the biomechanical mechanisms in teleost skulls (Anker, 1974; Lauder and Liem, 1981; Muller, 1987; Westneat, 1990). In unison, such studies have provided the functional understanding necessary to encapsulate the seemingly monumental diversity of teleost feeding patterns into two distinct modes (Liem, 1980; Ferry-Graham et al., 2002): a broad ram–suction group, covering all enveloping feeding methods (Lauder, 1980; Motta, 1982; Westneat and Wainwright, 1989; Wainwright and Shaw, 1999; Ferry-Graham et al., 2001b; Wainwright et al., 2001; Sanford and Wainwright, 2002; Svanbäck et al., 2002), and dislodging forms, which are often referred to as 'biters' (Barel, 1983; Motta, 1988; Turingan et al., 1995; Ferry-Graham et al., 2001c).

On coral reefs, recent studies have successfully documented the ecomorphological relationships between morphology of the feeding apparatus, associated prey-capture kinematics, behavioural performance and feeding ecology of both wrasses (f. Labridae) (Westneat, 1990; Sanderson, 1990; Clifton and Motta, 1998; Ferry-Graham et al., 2001c, 2002; Hulsey and Wainwright, 2002; Wainwright et al., 2004) and butterflyfishes (f. Chaetodontidae) (Motta, 1985, 1988, 1989; Ferry-Graham et al., 2001a,b). While insightful, these studies have concentrated predominantly on ram–suction feeding taxa, a continuum of feeding modes that are primarily associated with capture of free-living, loosely attached and/or delicate prey (Motta, 1988; Sanderson, 1990; Wainwright et al., 2004). Jaw closure kinematics associated with these feeding modes are generally considered inadequate for grabbing and dislodging firmly attached and/or structurally resilient prey (but see Ferry-Graham et al., 2002).

While a number of studies have examined structural

morphology in biting coral reef teleosts, these have focussed primarily on robust bioeroders and more gracile herbivorous or detritivorous taxa (Bellwood and Choat, 1990; Purcell and Bellwood, 1993; Bellwood, 1994; Bellwood, 2003; Alfaro et al., 2001; Ferry-Graham et al., 2002; Streelman et al., 2002). Such grazing, scraping and excavating forms predominate among surgeonfishes (f. Acanthuridae) and parrotfishes (f. Scaridae), where structural attributes of the feeding apparatus, e.g. degree of jaw robustness or motility, reflect microhabitat use and differential patterns of food procurement (Bellwood and Choat, 1990; Purcell and Bellwood, 1993). However, with the exception of labrids (including some scarids) (Alfaro et al., 2001; Ferry-Graham et al., 2001c, 2002; Westneat, 1990) and tetraodontiform fishes (Turingan et al., 1995) relatively little functional knowledge exists for biters, especially those that feed on structurally resilient and/or sturdily attached prey. Considering the prevalence of biting taxa on coral reefs, the paucity of information on both functional diversity and degree of complexity in morphology and kinematics underlying this assortment of feeding strategies stands out as a fundamental gap in our current understanding of feeding modes and their functional role in coral reef ecology (Wainwright and Bellwood, 2002).

The gracile and usually more derived biting taxa often possess an intramandibular joint (IMJ), a major morphological innovation that increases morphological as well as functional complexity by decoupling the mandible into two functional units and permitting rotation of the dentary on the articular. This may expand jaw gape, resulting in a larger area of substratum being contacted in each feeding event (Bellwood and Choat, 1990; Bellwood, 1994; Purcell and Bellwood, 1993; Streelman et al., 2002). While IMJ kinematics remain unquantified, IMJ presence also appears to be associated with changes in the orientation of the body and the jaws to the substratum (Bellwood et al., 2004), as well as the curvature of substratum utilised (Bellwood et al., 2003).

Of the coral reef teleosts putatively labelled as biters, the marine angelfishes (f. Pomacanthidae) form an interesting and hitherto neglected assemblage. Although taxonomically conservative (*c.* 80 spp.), they are iconic reef fishes with a circum-global distribution on tropical to warm-temperate reefs (Allen et al., 1998). Both pomacanthids and their well-studied sister family, the Chaetodontidae (Burgess, 1974) possess bristle-shaped teeth arranged in multi-tier arrays, which may provide exceptional gripping ability during feeding (Motta, 1989). Chaetodontids are known to possess a wide range of biomechanical specialisations associated with several trophic guilds (Motta, 1985, 1988; Ferry-Graham et al., 2001a,b) and a similarly wide range of trophic guilds has been inferred for pomacanthids (Allen, 1981; Allen et al., 1998; Debelius et al., 2003; Bellwood et al., 2004). While structural information exists (Gregory, 1933; Burgess, 1974), the functional aspects of pomacanthid feeding morphology and biomechanics have not been quantified (Wainwright and Bellwood, 2002). A recent molecular phylogeny has identified the large, robust omnivorous members of the genus *Pomacanthus* as the basal pomacanthid taxon (Bellwood et al., 2004). In contrast to the more derived pygmy angelfishes, which primarily target delicate prey items, *Pomacanthus* species feed on firmly attached and structurally resilient invertebrate components of the reef biota, including poriferans, tunicates, ascidians and soft corals (Allen, 1981; Allen et al., 1998; Debelius et al., 2003). These prey commonly favour confined and complex microhabitats (Richter et al., 2001), which raises the question: how are structurally resilient prey items reached, seized and dislodged from confined habitats when the large body size in *Pomacanthus* (sometimes 50–60 cm in total length) would appear to hinder this foraging strategy? No previously described functional system readily explains the microhabitat utilisation and feeding patterns of *Pomacanthus*, and the present study aims to quantitatively analyse the functional morphology, kinematics and performance characteristics of the feeding apparatus in this basal pomacanthid taxon to investigate the structural and functional basis of pomacanthid prey procurement. We hypothesise that the pomacanthid feeding apparatus contains novel functional diversity, and that the associated feeding kinematics match the diverging pomacanthid feeding guilds. Specifically, we test if *Pomacanthus* has a functional IMJ and, if so, whether intramandibular kinematics facilitates an extended gape angle as previously suggested in other IMJ-bearing taxa.

Materials and methods

Study taxon and specimen collection

The Koran angelfish *Pomacanthus semicirculatus* (Cuvier 1831), is one of the largest of its genus, attaining over 50 cm standard length (*SL*), and has uniformly pale head coloration, making it particularly suitable for motion analyses. This species has a wide distribution throughout the Indo-west Pacific, and is typically found in high complexity habitats with some vertical relief, where it feeds on structurally resilient attached prey, including sponges, tunicates, ascidians, soft corals and foliose calcareous or turf algae (Allen et al., 1998, N. Konow, unpublished). A total of 11 specimens (164–330 mm *SL*; 42–85 mm head length, *HL*) were collected with a barrier net from mid-shelf reefs on the Great Barrier Reef.

Dissections, manipulations and clear staining

Specimens for dissections were euthanized by immersion in seawater with an overdose of clove oil (Munday and Wilson, 1997), manipulated for identification of biomechanical linkages and frozen for dissection, or fixed in buffered 10% formaldehyde for clear-stain preparations and myology studies. Tissue clearing of fixed specimens (N=3) involved immersion in enzymatic pre-soak detergent (Gosztonyi, 1984) with subsequent KOH digestion and counter-staining for bone and cartilage, using a protocol modified from Dingerkus and Uhler (1977). Fixed specimens (N=7) were dissected to determine origin, insertion, fibre orientation and relative prominence of muscle complexes, as well as tendon, ligament

and connective tissue morphology. Cleared and stained specimens, as well as dissections of fresh specimens were used for manipulative studies, qualitatively examining biomechanical mechanisms adjoining the oral jaw, suspensorial and hyoid apparatus, with the neurocranium and pectoral girdle, during jaw protrusion, closure and retraction. During such manipulations, specimens were pinned to a reference grid background under a mounted digital camera, and step-photographed while the following manipulations were carried out (see numerical arrowhead labels for directions of manipulations in Fig. 1B). (1) Posterior-directed force applied to the urohyal (isthmus), imitating contraction of the m. sternohyoideus and m. hypaxiali, contributing to mandible depression in suction-feeders. (2) Posterior-directed force applied to the supraoccipital crest, imitating contraction of the m. epaxialis, causing cranial elevation and facilitating mandible protrusion in ram-feeders. (3) Caudal rotation of the ventral opercular margin, imitating contraction of the m. levator operculi, causing displacement of the opercular linkage, tightening the opercular-mandibular ligament (LIM), and contributing to mandible depression. (4) Anterodorsal displacement of the quadrate articular articulation, imitating contraction of the m. levator arcus palatini, causing anterior-directed suspensorial rotation, and augmenting mandible protrusion in some ram-feeders. (5) Dorsal rotation of the dentary with the articular fully depressed, imitating contraction of m. adductor mandibulae subsection 2 (A2), causing jaw closure. Anatomical and biomechanical diagrams were drawn directly from dissections using a camera lucida, or traced from digital stills of clear-stain preparations using Corel Draw v.10. (Corel Corp.). Osteology, myology and connective tissue nomenclature follows Winterbottom (1974) and Motta (1982).

Live specimen husbandry and experimental design

Specimens were held in individual experimental aquaria with shelter, at 26±2°C with a 12 h:12 h L:D photoperiod and screened from external visual stimuli with an opaque nylon cloth. All fish were acclimated for 1–2 weeks prior to experimentation. For provisioning as well as feeding trials, rock oyster shells of uniform size (5–6 cm^2 surface area) and covered with sponge, turf algae, ascidian, tubeworm and tunicate epifauna were collected from local coastal marine pylons. During acclimation, specimens were trained to feed under floodlight illumination on epifauna from shells clipped into a stainless steel crocodile beak on a steel wire shaft mounted in a 300 g polymer base.

Prior to video recording, specimens were anaesthetised by immersion in seawater with 1% clove oil in ethanol (Munday and Wilson, 1997). While anaesthetised, reflective markers were attached with cyano–acrylic glue to the skin to provide external topographic landmarks for biomechanical linkages in the oral jaws, suspensorium, cranium and pectoral girdle (Fig. 1). This procedure was completed in less than 100 s and caused no apparent stress, as specimens typically fed vigorously shortly after recovery from anaesthesia.

Sampling and analysis of kinematics

High-speed videography was completed over a 2–5 day period for each specimen, with a total of three specimens (*SL*=190, 245 and 330 mm; *HL*=51, 63 and 85 mm) being observed. All aquaria were equipped with 2 cm^2 reference grid backgrounds and illuminated with two 500 W halogen floodlights during video recording. Specimens were presented with attached prey in the gap between the aquarium front and the reference grid background, to ensure the specimen was perpendicular to the lens axis, and recorded using a JVC GR-DVL9800u digital video camera at 200 images s^{-1}. Video sequences were captured to a PC hard drive *via* a Canopus DV Raptor capture board and converted to raw AVI format in Virtual Dub v.1.0. Five feeding events for each specimen were selected for comprehensive analysis of feeding kinematics and to generate a performance profile of key components of the feeding apparatus. Each frame in selected sequences was separated to eight de-interlaced image fields, yielding stacks of 200 TIFF images s^{-1}, which were recompiled to AVI format in MatLab v.6.0 with resulting image stream resolution of 320×240 pixels. A further three specimens (*SL*=197, 241, 261 mm; *HL*=55, 61, 67 mm) were recorded using a 3Com single-CCD camera at 50 images s^{-1}. Sequences were captured real-time to hard drive using Pictureworks image recording software v. 2.0 and stored as AVI files for analysis. As this frame rate captured ~30 frames per feeding event, these sequences were only used for analysis of excursion maxima and velocity characteristics of feeding kinematics. All selected sequences were inspected in Virtual Dub and cropped from feeding event start (T_S) *via* protrusion onset (T_0) to maximum protrusion (T_{MAX}), bite (T_B) and feeding event conclusion (T_C). Onset of bite (T_{MAX}) coincided with maximum jaw gape and protrusion, with time of bite (T_B), being the frame showing jaw closure onto the prey. Sequences were submitted to analysis only if the full feeding event was completed in focus and in lateral profile. As performance maxima were the focus of this study, slow bites were rejected, as they appeared to result from predator hesitation. For the latter analyses, the high-speed sequences were subsampled at 50 images s^{-1} for standardisation and 10 feeding events for each of the six specimens filmed were analysed for maximum gape, maximum protrusion, and total feeding event duration (T_{TOT}). The contribution of body ram (R_B) and jaw ram (R_J, equalling R_B extracted from total ram, R_{TOT}) to prey approach were also recorded.

For the performance profile analysis, 13 reference points (Fig. 1), a target point (T) on the prey where the strike landed, and an origin reference on the grid-background (used to normalise data for image flicker and in the event of slight, unnoticed prey movement) were tracked in Movias Pro v.1.0 (Pixoft-NAC, 2002). Here, x:y coordinates were extracted for each reference point position in consecutive fields of the high-speed image stream. Visual inspection of video streams determined that protrusion duration varied more temporally than closure and retraction, and coordinate data columns from each bite were thus aligned to T_B, to minimise variation in

feeding kinematics. Excel macros were used to calculate vector lengths (distances between paired coordinate points) and angles between paired vectors (i.e. three coordinate points). Means ± S.E.M. of resulting values were plotted as incremental displacements (image-by-image, in 5 ms increments) of angles (Fig. 4) and linear distance (Fig. 5) between digitised points in *x*:*y* coordinate space. Onset-timing, magnitude and duration is illustrated for the following kinematic variables: total ram movement relative to the prey (R_{TOT}), from which body-ram movement (R_B) was deducted to isolate jaw-ram movement (R_J), jaw gape expansion, premaxillary protrusion, mandibular rotation and protrusion, intramandibular rotation, preopercular rotation (as a proxy for suspensorial movement), opercular rotation (as a proxy for opercular linkage displacement), cranial elevation and isthmus movement (as a proxy for hyoid depression).

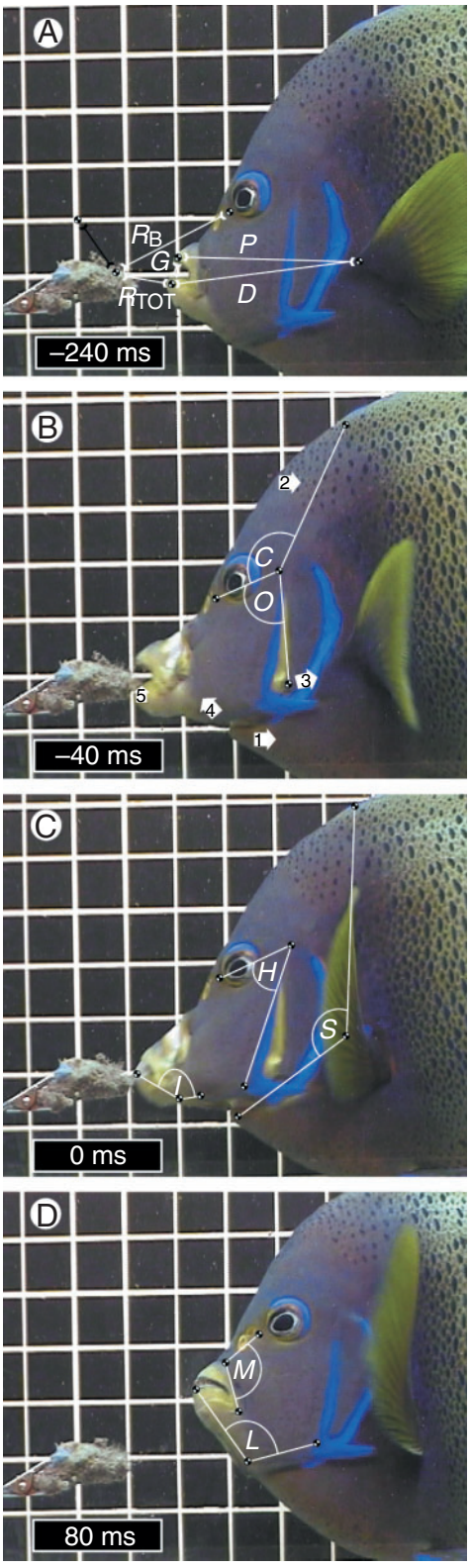

Fig. 1. High-speed image frames from a 200 frames s^{-1} recording illustrating the feeding event in a *Pomacanthus semicirculatus* specimen (245 mm *SL*) feeding on sponge attached to a clip. Reference grid squares are 2 cm^2, and time in ms from bite (T_B) in bottom left corner of frames: (A) protrusion onset; (B) maximum protrusion; (C) bite; (D) feeding event complete. Arrows with numerals (in B) refer to manipulations used on dissections (see text). Black and white dots indicate 15 landmarks on skull topography, prey and origin reference digitised in feeding sequences. Linear measurements (in A): R_{TOT}, total ram; R_B, body ram; *G*, gape distance; *P*, premaxilla excursion; *D*, dentary excursion. Black distance marker indicates origin-reference used to compensate for bite-related and unnoticed prey movements in analyses. Angular measurements (in B–D): *C*, cranial elevation; *O*, opercular rotation; *H*, suspensorial rotation; *S*, pectoral girdle rotation; *I*, intramandibular rotation; *M*, maxillary rotation; *L*, lower jaw depression.

Results

Feeding apparatus kinematics in *Pomacanthus* displays an unusual timing pattern (Fig. 3; see movie in supplementary material). After the preparatory and protrusion phases, the jaw closure phase precedes jaw retraction (Table 1). Specific kinematic profiles (Figs 4 and 5) and associated morphological specialisations (Fig. 2) for the three significant phases of a *Pomacanthus* feeding event (protrusion, closure and retraction) are described in sequence below.

Jaw protrusion

The hyomandibular bone and neurocranium have a synovial articulation on the ventral sphenotic margin (filled circle in Fig. 2A), which is associated with prominent adductor arcus palatini (AAP) and levator arcus palatini (LAP) musculature (Fig. 2B). Unusually, this permits anteroposterior movement of the hyomandibular, along with the closely associated elements of the suspensorium (Fig. 3A,B). Meanwhile, lateromedial expansion of the suspensorium remains comparable to other teleosts. The pterygoid series is reduced anteriorly with the palatine loosely suspended by connective tissue between the pterygoids and a cartilaginous pad on the lateral ethmoid (open circle in Fig. 2A). Anteriorly directed manipulation of the hyoid–hyomandibular mechanism (4 in Fig. 1B) results in a sliding of the palatopterygoid complex, and anterior movement of the suspensorium augmenting lower jaw protrusion (Fig. 3A,B). An interrupted pattern of suspensorial rotation is

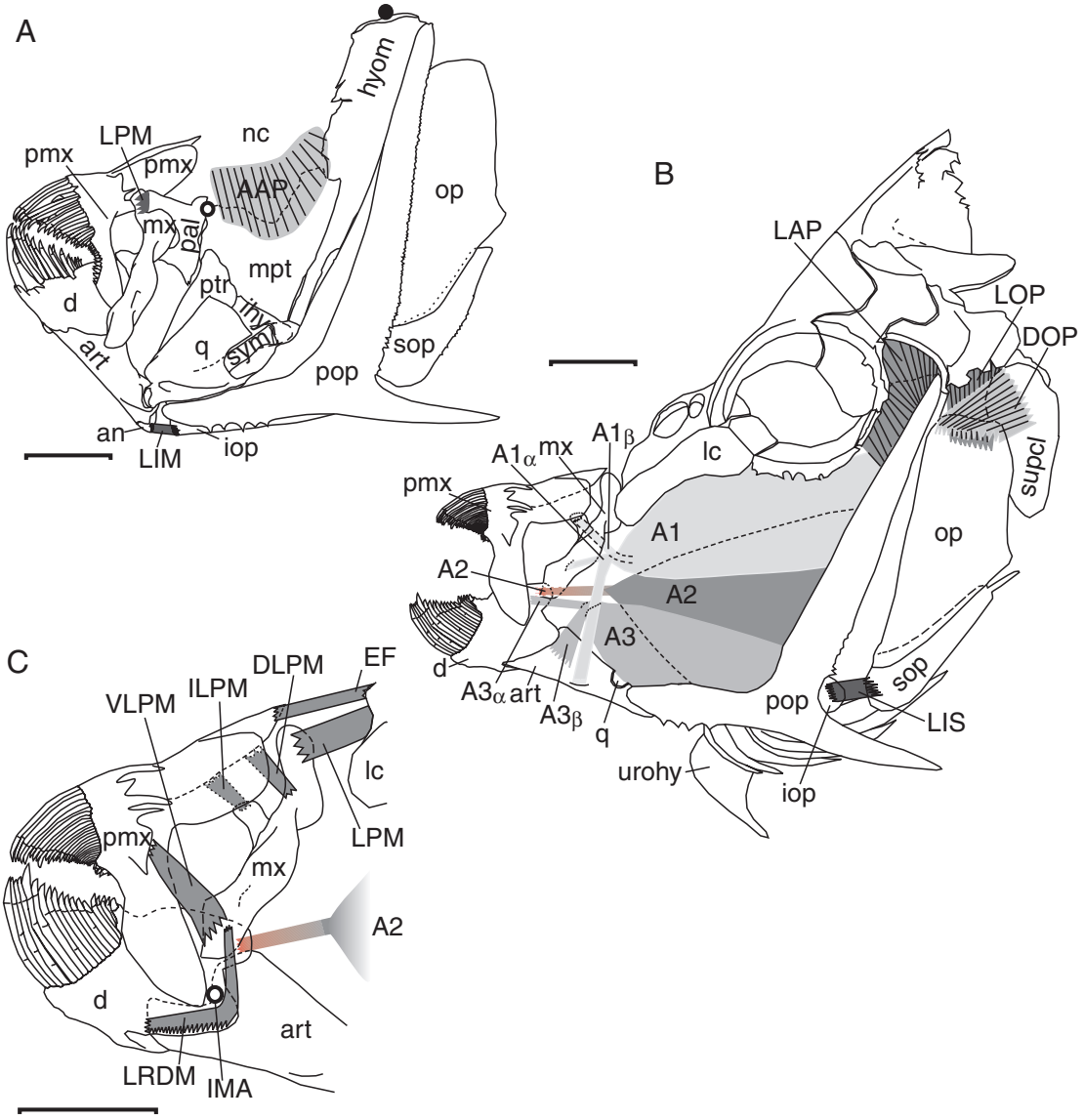

Fig. 2. Illustration of the *Pomacanthus semicirculatus* skull (left lateral view) based on clear-stained preparations. (A) Feeding apparatus when relaxed. (B) Suspensorium and operculum rotated, and jaws protruded. (C) Detail of protruded-closed oral jaws. Osteology labelling: an, angular; art, articular; d, dentary; hyom, hyomandibular; ihy, interhyal; iop, interoperculum; mpt, metapterygoid; mx, maxilla; op, operculum; pal, palatine; pmx, premaxilla; pop, preoperculum; ptr, ectopterygoid; q, quadrate; sop, suboperculum; supcl, supracleitrum; sym, symplectic; urohy, urohyal; lc, lachrymal; points of flexion are indicated in A between hyomandibular with nc, neurocranium (filled circle) and between the palatopterygoid complex of the suspensorium with the lateral ethmoid (open circle). Open circle in C: IMJ, intramandibular joint. Myology labelling: A1 (10% grey); A2 (50% grey, and medial to A1 and A3); A3 (30% grey), adductor mandibulae segments. LOP: levator operculi, DOP: dilator operculi, LAP: levator arcus palatini, AAP: adductor arcus palatini. Ligament labelling (all in 75% grey): EF, naso–premaxilla elastic fibres; DLPM, dorsal premaxilla–maxilla ligament; LIM, interopercular–mandibular ligament; LIS, interopercular–suboperculum ligament; ILPM, inner premaxilla–maxillary ligament; LPM, palatine–maxillary ligament; LRDM, articular–dentary–maxillary ligament; VLPM, ventral premaxilla–maxilla ligament. Scale bars, 10 mm.

seen (Fig. 1C, angle H; Fig. 4A), with an early rotation of ~4° initiating at T_B–600–500 ms, preceding all other feeding kinematics, and designating the feeding event start, T_S.

The mandible (Fig. 2A) consists of a compact dentary with an elongated, curved ventral process, a crescent-shaped coronoid process, and an exceptionally elongate articular, which effectively lowers the mandible–quadrate articulation fossa, and a distinct angular (retro–articular) bone. The articular descending process connects to the hyoid apparatus *via* a stout mandibular–basihyal ligament and to the opercular series *via* a prominent interopercular–mandibular ligament (LIM in Fig. 2A); no preopercular–mandibular ligament is present. The alveolar and ascending premaxillary processes are similarly elongate, and the laterally flattened maxilla has a prominent internal premaxillary condyle articulating with ridges on the premaxilla, and supported by a premaxillary–maxillary

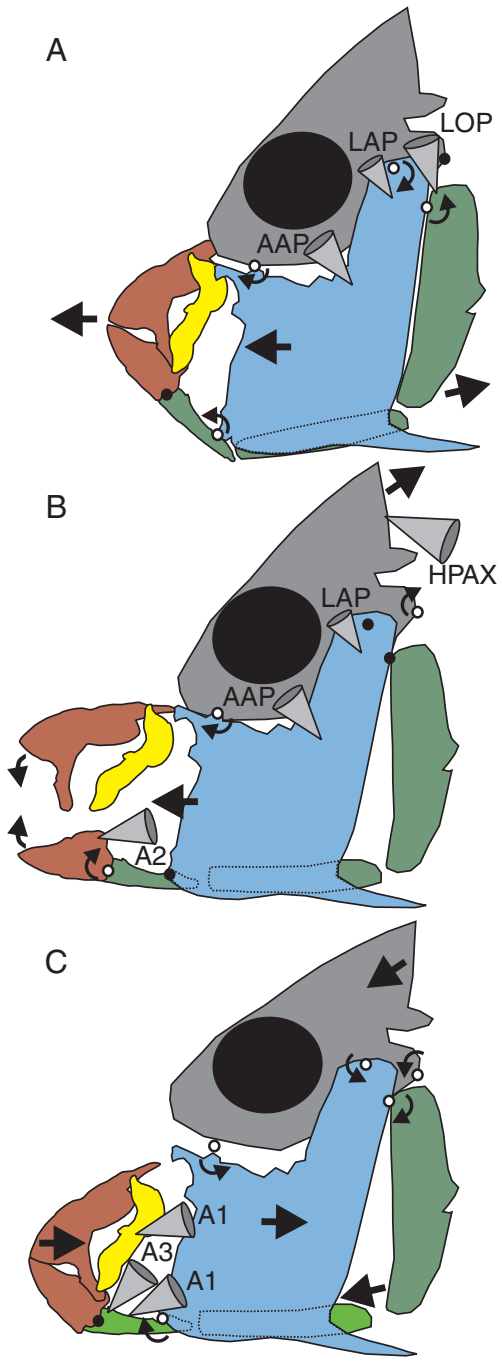

Fig. 3. Schematic figure of the skull kinematics of *Pomacanthus semicirculatus,* illustrating the three significant phases of a grab-and-tearing feeding event. (A) Jaw apparatus prior to protrusion onset, (B) protruded, and (C) protruded-closed state (upon jaw retraction, C returns to A after the recovery phase, in preparation for the next feeding event). Colour coding: grey, neurocranium, red, oral jaws, yellow, maxilla, blue, suspensorium, green, opercular series and articular. Arrows indicate displacement, mediated by tendons and ligaments. Open circles indicate rotation and filled circles indicate passive linkage. Cones represent inferred contraction of a muscle group, with myology labelling as in Fig. 2. HPAX: hypaxialis musculature.

ligament (LPM, in Fig. 2C). The anteroventrally tapering maxillary arm (Fig. 2A) has a reduced cranial condyle (compared with e.g. chaetodontids; Motta, 1982). Initial suspensorial rotation is followed by suspensorial stasis during *c.* 300 ms, while the onset of mandible depression (Fig. 1D, angle L; Fig. 4B at T_B–150 ms) augments gape expansion by rotation of ~38° (T_B–350 ms). Gape expansion coincides with a rotation of the operculum by ~8° (Fig. 1B, angle O; Fig. 4C), reaching maximum rotation around T_B–20 ms.

The opercular series (Fig. 2B) is formed by a vertical component, the fused operculum and suboperculum, which are

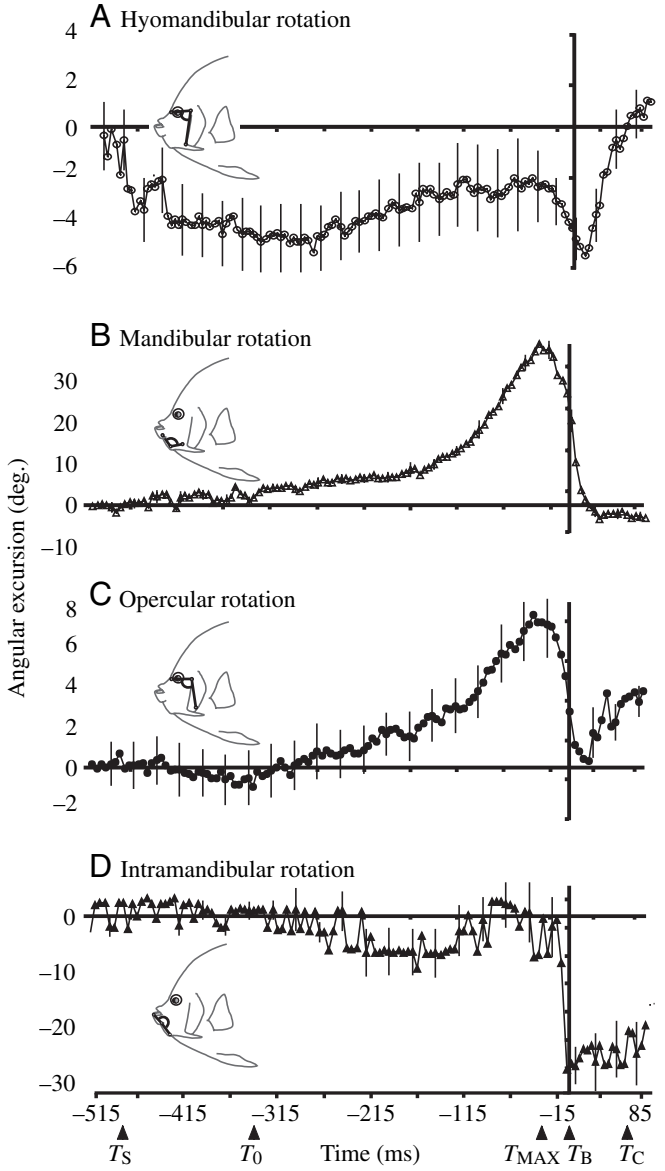

Fig. 4. Mean kinematics profiles for three *Pomacanthus semicirculatus* (five bites per individual, all bites pooled ± S.E.M.), illustrating timing of onset, magnitude and duration of angular displacement (in degrees) in: (A) hyomandibular; (B) mandibular; (C) opercular and (D) intramandibular mechanisms. Note the alignment of kinematics profiles around time of bite (T_B).

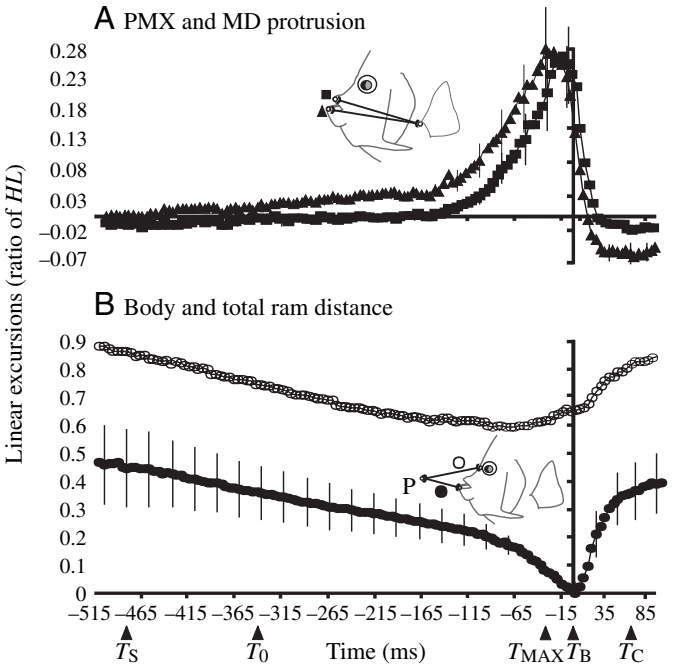

Fig. 5. Mean kinematics profiles for three *Pomacanthus semicirculatus* [five bites per individual, all bites pooled, vertical axis shows ratio of head length (*HL*) ± S.E.M.], illustrating timing of onset, magnitude and duration of linear displacement of: (A) the premaxilla (square) and the mandible (triangle); and (B) body-ram (open circle) and total-ram (closed circle).

connected by an interopercular-subopercular ligament (LIS) to the horizontally rectangular interoperculum, with a resting angle between mandible and interoperculum (Fig. 2A) of around 60°. Prominent LOP musculature can rotate the operculum around a synovial articulation on the dorsocaudal margin of the hyomandibular bone (Fig. 3A), mimicked by manipulating the ventral opercular margin, and the adjoined interoperculum in a dorsocaudal direction (3 in Fig. 1B). This displacement tightens the LIM (Fig. 2A), thereby causing mandible depression (Fig. 3A,B). As the oral jaws have a dorsally inclined resting position (Fig. 2A), due to extensive architectural reorganisation of the skull, the opercular series kinematics also causes rotational protrusion of the mandible (Fig. 3A,B). The hyoid apparatus is flexible, with reduced protractor hyoideus, sternohyoideus and genihyoideus musculature. Pectoral girdle rotation (measured as a proxy for hyoid depression, Fig. 1C, angle S) attains ~6.5°, around T_B–65 ms, with a prolonged duration. Similarly, the cranial articulation with the vertebra is mobile, with a raised supraoccipital crest enlarging the insertion surface for epaxial musculature. Cranial elevation (Fig. 1B, angle C) exhibits a slow and gradual increase to ~11°, with a peak around T_B–15 ms. In kinematics analyses, rotation in these two mechanisms are minimal around protrusion onset, only accelerating during the latter part of jaw protrusion. Despite the pronounced mobility in these mechanisms, neither isolated nor simultaneous manipulation (1 and 2 in Fig. 1B) resulted in mandible depression. The second stage of suspensorial rotation of ~4° (Fig. 4A) further augments mandible and premaxillary protrusion (|P| and |D| in Fig. 1A; Fig. 5A) and reaches maximum rotation around T_B.

Jaw closure

An intramandibular joint (IMJ) is present (Fig. 2C), with the lateral and medial walls of the dentary forming an articulating socket for the distal articular ascending process. Connective tissue restrains the dentary while allowing it to rotate on the articular, causing elevation of the tooth-bearing dentary surface. A single tendon from the medial A2 inserts into a deep medial fossa on the coronoid process of the dentary. No articular insertion of the A2 is present. The laterally convex, tooth-bearing surfaces of both the premaxilla and dentary contain tightly packed arrays of bristle-shaped teeth arranged in 5–7 tiers with tooth lengths decreasing posteriorly. A ventral premaxillary–maxillary ligament (VLPM in Fig. 2C), originating from the lateral premaxilla, inserts lateroventrally on the maxillary arm, while a prominent and modified articular–dentary–maxillary ligament (LRDM) connects the maxillary arm to almost the entire lateroventral surface of the dentary, but notably, not to the articular. Dentary manipulation (5 in Fig. 1B) causes tightening of this ligamentous array, forcing the tooth-bearing face of the premaxilla onto the dentary tooth face, resulting in mouth closure (Figs 1C, 3B,C), with the upper and lower jaw teeth occluding without superior or inferior overlap (Fig. 2C). Jaw closure kinematics (Fig. 3B) involve rotation of the intramandibular joint over ~5 ms, attaining ~30° (Fig. 1C, angle I, Fig. 4D), and occluding the protruded jaws at T_B.

Jaw retraction

The m. adductor mandibulae (Fig. 2B), while displaying the typical three divisions seen in teleosts, differs in some important respects. As noted above, a single tendon from the A2 inserts wholly on the dorsal surface of the dentary coronoid process. The A3 insertions are displaced posteriorly, away from the dentary, with one tendon from the ventrolateral A3α inserting in a shallow lateral fossa, while the medial A3β inserts on the sesamoid–articular, which is posteriorly displaced on the medial articular. The dorsolaterally situated A1 has two subsections: the A1α inserts onto the primordial ligament (the outer articular–maxillary ligament, or OLRM in Fig. 2B); the A1β inserts in a medial fossa on the premaxillary condyle of the maxilla. Jaw retraction (Fig. 3C) occurs with a slight lag (5 ms) after T_B (Fig. 1D, angle *L*; Fig. 5A), and is associated with a pronounced lateral head jerk. Reverse body movement at this time, caused by pectoral fin motion, yields an additional retraction of 20% *HL* from the prey (Fig. 5B). Jaw retraction kinematics is of high-velocity, encompassing 35° of mandible rotation and a linear excursion of ~30% *HL* over 20–60 ms, to complete the feeding event at T_C.

Feeding event velocity regimes and performance

Linear excursions of gape, jaw protrusion, jaw ram and body

Table 1. *Performance characteristics of prey-capture kinematics in* Pomacanthus semicirculatus

A

Ram variable	Distance	Maximum excursion (cm)	Velocity maxima (cm s^{-1})		
			Protrusion	Bite	Retraction
R_{TOT}	Total ram	7.2 (5.6)	11.6 (6.4)	2.3 (1.6)	99.6 (52.4)
R_J	Jaw ram	4.5 (2.9)	7.9 (4.8)	2.3 (1.6)	81.9 (45.0)
R_P	Body ram	2.0 (0.6)	5.4 (1.5)	0.01 (0.005)	31.7 (7.4)

B

Linear variable	Distance	Maximum excursion (*%HL*)	Onset (ms from T_B)	Maximum excursion (ms from T_B)	Duration (ms)	Prot (ms)	Ret (ms)
G	Gape	11	–345	–45	345	300	45
P	PMX protrusion	22	–150	–15	175	135	40
D	MD protrusion	29	–155	–30	185	125	60

C

Angular variable	Mechanism	Mean excursion (deg.)	Onset (ms from T_B)	Maximum excursion (ms from T_B)	Duration (ms)
C	Cranial	–11.2°	–455	–10	540
O	Opercular	7.4°	–290	–30	310
H	Hyomandibular	–6.5°	–575	10	755
S	Sternohyoid	3.1°	–515	–5	600
I	Intramandibular	–30.0°	–10	0	125
L	Mandibular	37.9°	–340	–25	450
M	Maxillary	17.5°	–250	–40	335

Performance characteristics of prey-capture kinematics in *Pomacanthus semicirculatus* with linear distances, angles and durations derived from high-speed video sequences of 30 separate feeding events (*N*=6 individuals with 10 bites each; all bites pooled for analysis). Linear, angular and ram variables follow Fig. 1. (A) Ram excursions and velocities are given for protrusion, bite and retraction as maximum values (mean values indicated in parentheses). (B) Gape and protrusion with excursion maxima, timing of onset and maximum excursion relative to T_B and total duration. (C) Angular excursions, with excursion means, timing of onset and maximum excursion relative to T_B and total duration.

Table 2. *Prey-capture performance characteristics in* Pomacanthus *compared with previously studied acanthurid (A) and labroid (L) taxa*

Taxa	Superorder	Feeding mode	Jaw protrusion (*%HL*)	Maximum jaw velocity (cm s^{-1})	Protrusion duration (ms)	Retraction duration (ms)	IMJ kinematics	Ref.
Pomacanthus	A	B	30	–82	550	60	closing	Present study
Ctenochaetus	A	B	6	–12	120	110	opening	Purcell and Bellwood, 1993
Astatotilapia	L	S	13	47	15	30	flexion	Aerts et al., 1987
Chaetodon	A	S	7	8	24	24	–	Motta, 1985, 1988
Forcipiger	A	R	30	13	30	40	–	Ferry-Graham et al., 2001a
Epibulus	L	R	65	230	35	76	–	Westneat and Wainwright, 1989
Petenia	L	R	55	65	24	–	–	Waltzek and Wainwright, 2003

Designation of feeding modes (B, biting; S, suction; R, ram). (*HL*, head length; IMJ, intramandibular joint). Note that all taxa except *Pomacanthus* lack a dedicated mechanism for protruded jaw closure, and negative values represent speeds attained during jaw retraction. While total bite duration in *Pomacanthus* bears most resemblance to other biters, the inverse intramandibular joint kinematics, magnitude of jaw protrusibility and velocity maxima distinguishes *Pomacanthus* from other biters; *Pomacanthus* kinematics values bear a stronger resemblance to ram feeders.

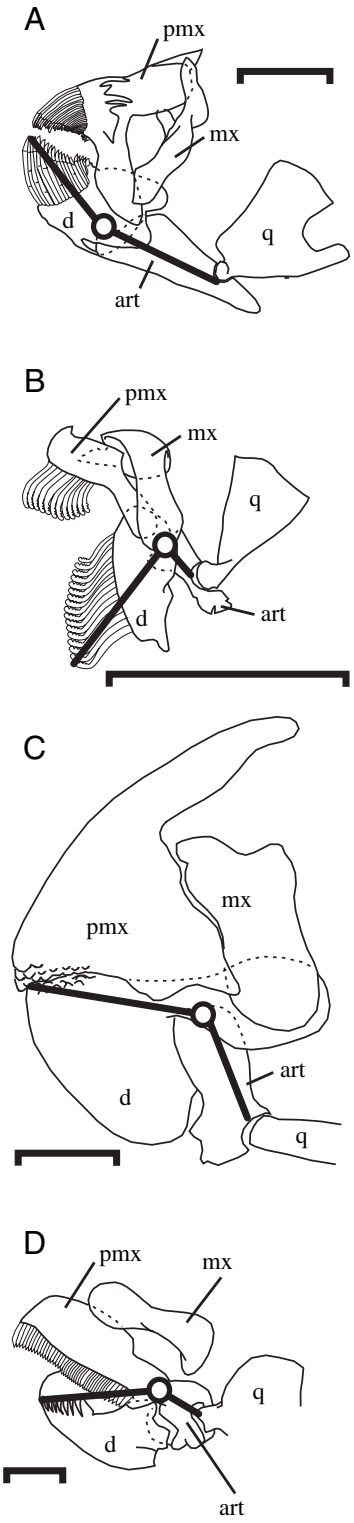

Fig. 6. Camera lucida drawings of the feeding apparatus in four biting coral reef teleosts with intramandibular joints marked by open circles. Proximal (articular) and distal (dentary) components of the joints are marked by solid black bars (see text for explanation). (A,B) joints rotated, (C,D) joints relaxed. (A) *Pomacanthus* (f. Pomacanthidae); (B) *Ctenochaetus*, (f. Acanthuridae); (C) *Scarus,* (f. Scaridae); (D) *Escenius,* (f. Blennidae). Scale bars, 10 mm, except D, 0.1 mm. Labelling follows Fig. 2.

ram are summarised in Table 1. Mandible protrusion (Fig. 1A, Δ|D|) attains about 30% *HL*, with subsequent retraction of the mandible beyond the resting point accounting for the negative protrusion values (Fig. 4E). Premaxillary protrusion (Fig. 1A, Δ|P|) attains ~27% *HL*, and occurs with an approximately 30 ms lag from mandible protrusion. During a feeding event, body ram, measured as the change in distance from prey to the nape (Fig. 1A, $\Delta|R_B|$) accounts for a 20% *HL* movement (Fig. 5B). Jaw protrusion is initiated outside a distance of 60% *HL* from the prey, and jaw-ram (Fig. 1A, $\Delta|R_{TOT}–R_B|$) typically covers ~30% *HL*. Body-ram velocities exhibit little change throughout the feeding event (Table 1); while the changes in jaw-ram velocity are notable (as visualised by varying curve slopes in Fig. 5B), with a slow protrusion (mean 6.4 cm s^{-1}), fast closure (mean 16.0 cm s^{-1}), and high-velocity retraction (mean 52.4 cm s^{-1}) during the feeding event phases (Table 1A). The conventional measurement of total bite duration ($T_C–T_0$) averages 450 ms, measured using jaw protrusion as proxy (Fig. 5A). However, when accounting for the early excursion of the suspensorium (Fig. 4A), mean bite duration ($T_C–T_S$) increases to about 600 ms, and sometimes approaches 750 ms (Table 2).

Discussion

The feeding apparatus morphology and associated feeding kinematics in *Pomacanthus* differ markedly from a generalised perciform suction feeder. In suction feeding taxa, onset of cranial elevation commonly coincides with onset of oral gape expansion and jaw protrusion, followed by hyoid retraction and/or depression, while jaw occlusion occurs at completion of jaw retraction (Wainwright and Shaw 1999; Alfaro et al., 2001; Grubich, 2001; Ferry-Graham et al., 2001c, 2002; Sanford and Wainwright, 2002). In *Pomacanthus*, however, (1) an intramandibular joint yields a novel sequence of onset timing in the retraction phase of the feeding event by facilitating protruded jaw closure; (2) steep resting angles enable the opercular mechanism to at least partially relieve the cranial elevation and hyoid depression in the initiation of mandible depression; (3) anteroposterior rotation in the hyomandibular–cranial articulation, combined with pronounced palatoethmoid and palatopterygoid flexion, facilitates suspensorial rotation, which precedes other mechanisms and augments mandible protrusion; (4) suspensorial and opercular linkage stasis upon jaw closure appears to stabilise the feeding apparatus for optimised bite-force tenacity; and (5) novel velocity regimes during the feeding event have great influence on feeding ecology.

The intramandibular joint

In an early descriptive account, Gregory (1933) noted "an incipient articulation of the dentary in the lower jaw of *Angelichthyes*" [*Holacanthus ciliaris*], but did not elaborate on functional implications, or the presence of intramandibular joints in other pomacanthids. In fact, intramandibular articulation may be the most significant morphological

specialisation in the feeding apparatus of pomacanthids, with drastic consequences for feeding kinematics. Whilst bearing strong anatomical resemblance to IMJs described in other biting taxa (Fig. 6), the IMJ kinematics of *Pomacanthus* appear to be unique. In at least two acanthurid genera (*Acanthurus* and *Ctenochaetus;* Purcell and Bellwood, 1993) and three scarid genera (*Chlorurus*, *Hipposcarus* and *Scarus;* Bellwood, 1994; Streelman et al., 2002), IMJ kinematics, although unquantified, appear to increase gape expansion and function while the jaws are retracted. In *Pomacanthus*, however, IMJ kinematics produce jaw closure with the mandible maximally depressed and the jaws at peak protrusion (Fig. 3). As a result, a distinct closing stage is added prior to the retraction phase of the feeding event, contrasting with the feeding kinematics in other IMJ bearers, as well as in perciform teleosts as a whole (Table 2; Ferry-Graham and Lauder, 2001).

Alternative mechanisms of mandible depression and jaw protrusion

Mandible depression kinematics in *Pomacanthus* appears to be driven by opercular rotation, thus differing from many other teleosts, and especially suction and ram-feeders, in which cranial and/or hyoid kinematics have an early onset (Muller, 1987; Aerts et al., 1987; Alfaro et al., 2001). In more basal fishes the cranial/hyoid mechanisms are considered functional alternatives to the opercular linkage for initiation of mandible depression (Lauder, 1980; Carroll and Wainwright, 2003). However, our kinematic results as well as morphological properties of the *Pomacanthus* feeding apparatus suggest an inferior importance of these mechanisms in angelfishes. The onset timing of cranial elevation is delayed and during jaw opening the hyoid apparatus does not protrude ventrally (anterior to the isthmus in Fig. 1) as is typically the case in suction-feeders utilising this linkage (Motta, 1982; Aerts et al., 1987).

Hyoid myology appears to be reduced compared with chaetodontids (Motta, 1982), yet the hyoid apparatus appears to be more flexible (Burgess, 1974; Motta, 1982). Our manipulation studies of the *Pomacanthus* feeding apparatus demonstrate that the oral jaws, suspensorium and opercular series constitute a functionally discrete unit, with component parts being capable of generating mandible depression, gape expansion and oral jaw protrusion/retraction. The resultant displacements are of magnitudes comparable to those obtained in video kinematics yet exclude input from the hyoid and cranial linkages. The observed lag in premaxillary protrusion, suggests that premaxillary kinematics is driven by that of the mandible, corresponding with a ‘type-B protrusion mechanism’ (*sensu* Winterbottom, 1974; see also Motta, 1984). Pomacanthids are unusual in having the oral jaws resting with a dorsal inclination relative to the interoperculum, which rests at a steep angle to the operculum (Gregory, 1933). Articular elongation increases the mandible out-lever, while anterior displacement of the quadrate articulation leaves the proximal articular as a hypertrophied opening in-lever (Fig. 6). Combined, these traits may provide the biomechanical leverage to make opercular rotation the primary mechanism responsible for mandible depression and premaxillary protrusion (Anker, 1974).

Several lines of evidence support this interpretation, including the synchrony observed in opercular rotation and mandible depression kinematics (Fig. 4), and the presence of well developed LOP musculature. Most labroids (including the extreme jaw-protruders) have an opercular–mandibular resting angle around 0°, and less developed opercular musculature (Wainwright et al., 2004; N.K., unpublished). It is perhaps for this reason that opercular rotation has been considered of inferior importance when compared with the role of cranial elevation for initiation of mandible depression in teleosts (Westneat, 1990). Still, both Anker (1974) and Motta (1982) suggested that the opercular mechanism provided significant input to mandible depression initiation in several suction-feeding taxa. More recent experimental studies on suction-feeding cichlids and centropomids have shown drastically reduced mandible depression performance after surgical severance of the interopercular–subopercular ligament (LIS: in Fig. 2A) while leaving the LIM, with the opercular–hyoid connection intact (Durie and Turingan, 2004; R. Turingan, personal communication). While the opercular mechanism may well represent a functional reversal to a basal teleost mechanism, dominant in Halecostome fishes and retained in some extant larval teleosts (Adriaens et al., 2001; Lauder and Liem, 1981), it is noteworthy that similar opercular–mandibular angles are observed in other biting taxa (Fig. 6), both closely (*Acanthurus* and *Ctenochaetus*) and more distantly (*Scarus*) related. Given the paucity of kinematics data on biters, it remains unclear if a functional opercular mechanism is a shared trait among biters.

Within and between-mode performance variations

Mandible protrusion of 30% *HL*, as observed in *Pomacanthus,* may be considered extreme, and is a rare trait in teleosts. Such protrusion magnitude was previously only described in the cichlid genera *Petenia* and *Caquetaia* (Waltzek and Wainwright, 2003), the chaetodontid *Forcipiger* (Ferry-Graham et al., 2001a,b; Motta, 1984), and the labrid *Epibulus* (Westneat and Wainwright, 1989). These taxa are all ram–suction feeders, possess extreme axial elongation of several feeding apparatus elements, and complex suspensorial mechanisms, either based on pivoting elements (*Epibulus, Petenia* and *Caquetaia*) or suspensorial rotation around multiple points of flexion (*Forcipiger*). By comparison, *Pomacanthus* has suspensorial rotation around two novel points of flexion, contributing approximately 40% of the observed mandibular protrusion while depression of the dorsally inclined mandible contributes the remaining 60%. Axial bone elongation in *Pomacanthus*, albeit less pronounced than in other extreme jaw-protruders, is considerable in chaetodontoid terms (Motta, 1985, 1988). The resultant protrusion is of comparable magnitude to *Forcipiger*, for example, which displays the most extensive axial elongation of jaw osteology known in teleosts and three novel points

of suspensorial flexion (Table 2). In contrast, the hyomandibular–cranial articulation of scarid and acanthurid IMJ-bearers lack anteroposterior rotation, and the palatoethmoid region shows little flexion and no reduction. Indeed little or no mandibular protrusion has been documented in these taxa (Purcell and Bellwood, 1993; Bellwood, 1994; Motta, 1982), while in *Ctenochaetus*, modest suspensorial rotation appears to be coupled with gape angle and expansion increase rather than mandible protrusion (Purcell and Bellwood, 1993).

The differences in axial bone elongation and incidence of derived mechanisms in the feeding apparatus of *Pomacanthus* and other extreme jaw-protruders may reflect diverging structural requirements of ram–suction and biting kinematics during feeding (Table 2). In long-jawed ram–suction feeders, the prioritising of protrusion speed over jaw closure force (Barel, 1983) makes an axially elongated jaw apparatus a logical prerequisite, providing stability in order to maintain precision during the dramatic, high-velocity protrusion kinematics (Westneat and Wainwright, 1989; Waltzek and Wainwright, 2003). Conversely, in *Pomacanthus*, peak-protruded jaw closure and jaw retraction appear to be critical feeding kinematics. The initial suspensorial rotation stage is followed by a prolonged stage (350 ms) of partially rotated, static posture. The second rotation stage, occurs immediately prior to jaw closure (T_B–15 ms), and coincides with maximal rotation of the opercular-, cranial- and hyoid linkages. This late-protrusion constriction of the feeding apparatus presumably results from contraction of opercular, suspensorial, epaxialis and hypaxialis musculature and may serve to stabilise the oral jaw apparatus, thereby optimising the input from A2 contraction to dentary rotation, with a resultant direct force transmission for jaw closure. The close apposition of the hyomandibular bars, resulting from lateromedial skull compression, is an additional trait likely to govern bite forcefulness (Aerts, 1991).

Interestingly, while *Pomacanthus* jaw protrusion velocity is very slow (Table 1), mandible retraction velocity (approaching 100 cm s^{-1}) surpasses the high-velocity jaw movements of many ram feeders (Table 2). High retraction velocity corresponds well with the caudal displacement of A1 and A3 insertions. This displacement also leaves the A2 as the sole muscle rotating the dentary around the IMJ. Currently, anterior four-bar linkage models (Westneat, 1990; Hulsey and Wainwright, 2002; Wainwright et al., 2004) as well as models for mandibular mechanical advantage (Turingan et al., 1995; Wainwright and Shaw, 1999; Wainwright and Bellwood, 2002; Bellwood, 2003; Wainwright et al., 2004) do not allow for IMJ presence (Wainwright et al., 2004). The transmission coefficients of jaws with an IMJ are therefore unknown at present. However, it is noteworthy that *Pomacanthus* appears to be unique among IMJ-bearing teleosts in having the distal (dentary) portion of the IMJ equal to or longer than the proximal (articular) portion (Fig. 6). Whether this is causally related to pomacanthids being the only taxa with a closing IMJ remains to be determined.

Prey dislodgement force requirements could be met *via* alternative pathways, as mechanical output is not always linearly coupled with muscle contraction (Aerts et al., 1987). At jaw occlusion the prey is clenched between tiered bristle tooth rows in the protruded oral jaws, potentially with considerable gripping qualities. The protruded oral jaws appear to be stabilised in protruded-closed configuration by a rigid frame formed by the suspensorial and opercular rotation. A slight lag (5–7 ms) is observed prior to mandible retraction. It remains to be tested if this lag represents a stage of strain-energy storage in the m. adductor mandibulae sections involved with mandible retraction. Such an ‘elastic recoil mechanism’ was described in the mandible kinematics of *Astatotilapia*, where the power requirement for kinematics at the observed velocity exceeded the physical capability of mechanical output calculated from available muscle mass (Aerts et al., 1987). In *Pomacanthus*, cranial stabilisation during the pre-retraction lag may be preventing jaw retraction initiation, thereby augmenting strain-energy build-up in the A1 and A3 musculature, which is mobilised upon skull musculature relaxation (bar the A2). Trade-offs between forcefulness and rapidity during *Pomacanthus* mandible retraction, along with the functional properties of tiered bristle tooth rows, require further investigation. Further biomechanical modelling and tensiometry combined with EMG appear to be the most promising avenues for future research.

Ecological implications of intramandibular joints

While the IMJ of *Pomacanthus* structurally resembles that found in other biters, both the IMJ kinematics and the feeding ecology differ markedly. Only IMJs with inferred gape-expanding kinematics have previously been described in coral reef fishes (Fig. 6), such as the Acanthuridae (Purcell and Bellwood, 1993), the Scaridae (Bellwood 1994; Streelman et al., 2002) and in the blennid genus *Escenius* (N. Konow, unpublished). These taxa predominately graze or scrape planar or convex substrata (Choat and Bellwood, 1985; Bellwood et al., 2003; Depczynski and Bellwood, 2003). Hence, IMJ presence in *Pomacanthus* corresponds well with previous notions of biters exhibiting increased structural complexity in feeding apparatus morphology in accordance with the biomechanical challenges imposed by the substratum utilised (Wainwright and Bellwood, 2002). However, the unique IMJ kinematics of pomacanthids apparently relate to distinct ecological patterns of prey-capture (grab-and-tearing), reflecting a novel, but unquantified, pattern of microhabitat utilisation.

The unusual IMJ kinematics may be particularly important in the larger, spongivorous taxa, such as *Pomacanthus,* which prey on a wide range of invertebrate taxa, including sponges (Burns et al., 2003), gorgonians (Fenical and Pawlik, 1991) and soft corals (Wylie and Paul, 1989). These prey-taxa typically possess potent predator-deterring toxins (Wylie and Paul, 1989), leading previous workers to the assumption that chemical defence may be the primary basis for predation

deterrence in these important components of the non-coralline benthic reef community (Dunlap and Pawlik, 1996). Sponge toxin concentrations correlate well with the degree of within-habitat exposure to predation (Swearingen and Pawlik, 1998). Chaetodontoid fishes appear to utilise toxic prey through presumed tolerance of toxins (Wylie and Paul, 1989; Dunlap and Pawlik, 1996; Gleibs and Mebs, 1999; Thacker et al., 1998), but a complementary explanation may exist: many of the less exposed (and less toxic) invertebrate taxa also exhibit less structural resilience, and while it is likely that chemical and structural defences work in concert to reduce predation, as commonly seen in algae (Hay, 1992), trade-offs may exist between toughness and crypsis for many of the taxa consumed by pomacanthids. The result may be that the least structurally defended species exhibit the most cryptic lifestyles, and that the distribution and abundance of such invertebrate taxa is shaped by the abundance of predators with jaw protrusibility, coupled with a grab and tearing force sufficient enough to utilise such cryptobenthic resources. Other predators robust enough to dislodge these taxa may simply be unable to reach them due to large body size. This opens an interesting avenue of ecological research into the relative importance of large angelfish taxa in shaping the distribution and abundance of toxic and/or structurally resilient, cryptobenthic reef taxa.

Microhabitat utilisation in *Pomacanthus* contrasts markedly with most other coral reef fishes that feed predominantly on either free-living (ram–suction feeders), or attached prey on convex or planar surfaces (biters). The unique microhabitat utilisation patterns in *Pomacanthus* are apparently facilitated by several unusual kinematic characteristics, all bearing more resemblance to ram-feeders than to other biters (Table 2). As in long-jawed butterflyfishes, which are known to ram-feed on elusive non-attached prey in confined microhabitats, *Pomacanthus* exhibit extensive oral-jaw protrusion, enabling them to reach prey in complex and confined microhabitats. The unique IMJ kinematics, yielding peak-protruded jaw closure, combines with the prehensile properties of tiered bristle tooth rows, to reach concavities and obtain a high-tenacity grip on prey. Finally, the abrupt and high-velocity kinematics of jaw retraction, along with reverse body acceleration caused by pectoral fin and cranial movements, generates sufficient tearing strength and/or momentum to dislodge prey with pronounced structural resilience. These distinct traits, coupled with the characteristic repetitive-bite foraging pattern observed in spongivorous angelfishes suggest these taxa represent a functionally, as well as ecologically, distinct component of reef assemblages. Overall, the prey-capture kinematics of *Pomacanthus* differs markedly from other biters and, accordingly, their feeding activity should be considered as a new grab-and-tearing subcategory. How widespread this trait is within the Pomacanthidae, as well as in other teleost taxa, remains to be evaluated. However, the diversity of pomacanthid feeding guilds (Bellwood et al., 2004) suggests that we may find considerable functional diversity within this family.

Our thanks to staff at the Orpheus Island, One Tree Island and Lizard Island Research Stations; staff at MARFU (JCU); P. Hansen, A. Teitelbaum, S. Walker, L. Bay and G. Diaz for field assistance; J. Robinson (Pixoft, UK) for Movias Pro software; W. Mallet for high-speed image re-alignment code; C. Fulton, J. Moore, R. Fox and two anonymous reviewers for useful comments and discussions. This research was conducted in accordance with Great Barrier Reef Marine Park Authority research permit # G01/257 and James Cook University Ethics Approval # A657/01, and was supported by the Danish Research Agency, the Australian Coral Reef Society (N.K.) and the Australian Research Council (D.R.B.). Centre for Coral Reef Biodiversity contribution no. 139.

References

Adriaens, D., Aerts, P. and Verraes, W. (2001). Ontogenetic shift in mouth opening mechanisms in a catfish (Clariidae, Siluriformes): a response to increasing functional demands. *J. Morph.* **247**, 197-216.

Aerts, P. (1991). Hyoid morphology and movements relative to abducting forces during feeding in *Astatotilapia elegans* (Teleostei, Cichlidae). *J. Morph*. **208**, 323-345.

Aerts, P., Osse, J. W. M. and Verraes, W. (1987). Model of jaw depression during feeding in *Astatotilapia elegans* (Teleostei, Cichlidae): mechanisms for energy storage and triggering. *J. Morph.* **194**, 85-109.

Alfaro, M. E., Janovetz, J. and Westneat, M. W. (2001). Motor control across trophic strategies: muscle activity of biting and suction feeding fishes. *Am. Zool.* **41**, 1266-1279.

Allen, G. R. (1981). *Butterfly and Angelfishes of the World*. Vol. 2 (2nd edn) (ed. H. A. Baensch). Melle, Germany: Mergus.

Allen, G. R., Steene, R. and Allen, M. (1998). *A Guide to Angelfishes and Butterflyfishes*. Perth: Odyssey Publishing.

Anker, G. C. (1974). Morphology and kinetics of the head of the stickleback, *Gasterosteus aculeatus*. *Trans. Zool. Soc. Lond.* **32**, 311-416.

Barel, C. D. N. (1983). Towards a constructional morphology of Cichlid fishes (Teleostei, Perciformes). *Neth. J. Zool.* **33**, 357-417.

Bellwood, D. R. (1994). A phylogenetic study of the parrotfishes family Scaridae (Pisces: Labroidei), with a revision of genera. *Rec. Aust. Mus*. Suppl. **20**, 1-86.

Bellwood, D. R. (2003). Origins and escalation of herbivory in fishes: a functional perspective. *Palaeobiology* **29**, 71-83

Bellwood, D. R. and Choat, J. H. (1990). A functional analysis of grazing in parrotfishes (family Scaridae): the ecological implications. *Env. Biol. Fish*. **28**, 189-214.

Bellwood, D. R., van Herwerden, L. and Konow, N. (2004). Evolution and biogeography of marine angelfishes (Pisces: Pomacanthidae). *Mol. Phylogen. Evol*. **33**, 140-155.

Bellwood, D. R., Hoey, A. S. and Choat, J. H. (2003). Limited functional redundancy in high diversity systems: resilience and ecosystem function on coral reefs. *Ecol. Lett*. **6**, 281-285.

Burgess, W. E. (1974). Evidence for elevation to family status of the angelfishes (Pomacanthidae), previously considered to be a subfamily of the butterflyfishes (Chaetodontidae). *Pac. Sci.* **28**, 57-71.

Burns, E., Ifrach, I., Carmeli, S., Pawlik, J. R. and Ilan, M. (2003). Comparison of anti-predatory defenses of Red Sea and Caribbean sponges. I. Chemical defense. *Mar. Ecol. Prog. Ser.* **252**, 105-114.

Carroll, A. M. and Wainwright, P. C. (2003). Functional morphology of prey capture in the sturgeon, *Scaphirhynchus sapidus*. *J. Morph*. **256**, 270-284.

Choat, J. H. and Bellwood, D. R. (1985). Interactions among herbivorous fishes on a coral reef: influence of spatial variation. *Mar. Biol.* **89**, 221-234.

Clifton, K. B. and Motta, P. J. (1998). Feeding morphology, diet and ecomorphological relationships among five Caribbean labrids (Teleostei, Labridae). *Copeia* **4**, 953-966.

Debelius, H., Tanaka, H. and Kuiter, R. H. (2003). Angelfishes, a comprehensive guide to Pomacanthidae. Chorley, UK: TMC Publishing.

Depczynski, M. and Bellwood, D. R. (2003). The role of cryptobenthic reef fishes in coral reef trophodynamics *Mar. Ecol. Prog. Ser*. **256**, 183-191.

Dingerkus, G. and Uhler, L. D. (1977). Enzyme clearing of alcian blue

stained whole small vertebrates for demonstration of cartilage. *Stain Tech*. **52**, 229-232.

Dunlap, M. and Pawlik J. R. (1996). Video-monitored predation by Caribbean reef fishes on an array of mangrove and reef sponges. *Mar. Biol.* **126**, 117-123.

Durie, C. J. and Turingan, R. G. (2004). The effects of opercular linkage disruption on prey-capture kinematics in the teleost fish *Sarotherodon melanotheron*. *J. Exp. Zool. A* **301**, 642-653.

Fenical, W. and Pawlik, J. R. (1991). Defensive properties of secondary metabolites from the Caribbean gorgonian coral *Erythropodium caribaeorum*. *Mar. Ecol. Prog. Ser.* **75**, 1-8.

Ferry-Graham, L. A. and Lauder, G. V. (2001). Aquatic prey capture in ray-finned fishes: a century of progress and new directions. *J. Morph.* **248**, 99-119.

Ferry-Graham, L. A., Wainwright, P. C., Westneat, M. W. and Bellwood, D. R. (2002). Mechanisms of benthic prey capture in wrasses (Labridae). *Mar. Biol*. **141**, 819-830.

Ferry-Graham, L. A., Wainwright, P. C. and Bellwood, D. R. (2001a). Prey capture in long-jawed butterflyfishes (Chaetodontidae): the functional basis of novel feeding habits. *J. Exp. Mar. Biol. Ecol.* **256**, 167-184.

Ferry-Graham, L. A., Wainwright, P. C., Hulsey, C. D. and Bellwood, D. R. (2001b). Evolution and mechanics of long jaws in butterflyfishes (Family Chaetodontidae). *J. Morph*. **248**, 120-143.

Ferry-Graham, L. A., Wainwright, P. C., Westneat, M. W. and Bellwood, D. R. (2001c). Modulation of prey capture kinematics in the cheeklined wrasse *Oxychelinus diagrammus* (Teleostei: Labridae) *J. Exp. Zool.* **290**, 88-100.

Gleibs, S. and Mebs, D. (1999). Distribution and sequestration of palytoxin in coral reef animals. *Toxicon* **37**, 1521-1527.

Gosztonyi, A. E. (1984). The use of enzyme-based laundry presoaks for clearing small vertebrates for alizarin red staining of bony tissues. *Stain Tech.* **59**, 305-307.

Gregory, W. K. (1933). Fish skulls. A study of the evolution of natural mechanisms. *Am. Phil. Soc.* **23**, 1-468.

Grubich, J. R. (2001). Prey capture in actinopterygian fishes: a review of suction feeding motor patterns with new evidence from an elopomorph fish, *Megalops atlanticus*. *Am. Zool*. **41**, 1258-1265.

Hay, M. E. (1992). Fish-seaweed interactions on coral reefs: effects of herbivorous fishes and adaptations of their prey. In *The Ecology of Fishes on Coral Reefs* (ed. P. F. Sale), p. 96-119. San Diego, USA: Academic Press.

Hulsey, C. D. and Wainwright, P. C. (2002). Projecting mechanics into morphospace: disparity in the feeding system of labrid fishes. *Proc. Roy. Soc. Lond. Ser. B* **269**, 317-326.

Lauder, G. V. (1980). Evolution of the feeding mechanism in primitive actinopterygian fishes: a functional anatomical analysis of *Polypterus, Lepisosteus* and *Amia*. *Copeia* **1981**, 154-168.

Lauder, G. V. and Liem, K. F. (1981). Prey capture of *Luciocephalus pulcher*. Implications for models of jaw protrusion in teleost fishes. *Env. Biol. Fish.* **6**, 257-268.

Liem, K. F. (1980). Acquisition of energy by teleosts: adaptive mechanisms and evolutionary patterns. In *Environmental Physiology of Fishes*, vol. 35 (ed. M. A. Ali), pp. 299-334. New York, London: Plenum Press.

Motta, P. J. (1982). Functional morphology of the head of the inertial suction feeding butterflyfish, *Chaetodon miliaris* (Perciformes, Chaetodontidae). *J. Morph*. **174**, 283-312.

Motta, P. J. (1984). The mechanics and functions of jaw protrusion in teleost fishes: a review. *Copeia*. **1984**, 1-18.

Motta, P. J. (1985). Functional morphology of the head of Hawaiian and Mid-Pacific butterflyfishes (Perciformes, Chaetodontidae). *Env. Biol. Fish*. **13**, 253-276.

Motta, P. J. (1988). Functional morphology of the feeding apparatus of ten species of butterflyfishes (Perciformes, Chaetodontidae) an ecomorphological approach. *Env. Biol. Fish.* **22**, 39-67.

Motta, P. J. (1989). Dentition patterns among Pacific and Western Atlantic butterflyfishes (Perciformes, Chaetodontidae): relationship to feeding ecology and evolutionary history. *Env. Biol. Fish*. **25**, 159-170.

Muller, M. (1987). Optimization principles applied to the mechanism of neurocranium levation and mouth bottom depression in bony fishes (Halecostomi). *J. Theor. Biol*. **126**, 343-368.

Munday, P. L. and Wilson, S. K. (1997). Comparative efficacy of clove oil and other chemicals in anaesthetization of *Pomacentrus amboinensis*, a coral reef fish. *J. Fish Biol*. **51**, 931-938.

Purcell, S. W. and Bellwood, D. R. (1993). A functional analysis of food procurement in two surgeonfish species, *Acanthurus nigrofuscus* and *Ctenochaetus striatus* (Acanthuridae). *Env. Biol. Fish*. **37**, 139-159.

Richter, C., Wunsch, M., Rasheed, M., Kotter, I. and Badran, M. I. (2001). Endoscopic exploration of Red Sea coral reefs reveals dense populations of cavity-dwelling sponges. *Nature* **6857**, 726-730.

Sanderson, S. L. (1990). Versatility and specialization in labrid fishes: ecomorphological implications. *Oecologia* **84**, 272-279.

Sanford, P. J. and Wainwright, P. C. (2002). Use of sonomicrometry demonstrates the link between prey capture kinematics and suction pressure in largemouth bass. *J. Exp. Biol.* **205**, 3445-3457.

Streelman, J. T., Alfaro, M., Westneat, M. W., Bellwood, D. R. and Karl, S. A. (2002). Evolutionary history of the parrotfishes: biogeography, ecomorphology and comparative diversity. *Evolution* **56**, 961-971.

Svanbäck, R., Wainwright, P. C. and Ferry-Graham, L. A. (2002). Linking cranial kinematics, buccal pressure and suction feeding performance in largemouth bass. *Physiol. Biochem. Zool.* **75**, 532-543.

Swearingen, D. C., III and Pawlik, J. R. (1998). Variability in the chemical defence of the sponge *Chondrilla nucula* against predatory reef fishes. *Mar. Biol.* **131**, 619-627.

Thacker, R. W., Becerro, M. A., Lumbang, W. A. and Paul, V. J. (1998). Allelopathic interactions between sponges on a tropical coral reef. *Ecology* **79**, 1740-1750.

Turingan, R. G., Wainwright, P. C. and Hensley, D. A. (1995). Interpopulation variation in prey use and feeding biomechanics in Caribbean triggerfish. *Oecologia* **102**, 296-304.

Wainwright, P. C. and Bellwood, D. R. (2002). Ecomorphology of feeding in coral reef fishes. In *Coral Reef Fishes. Dynamics and Diversity in a Complex Ecosystem* (ed. P. F. Sale), pp. 32-55. San Diego: Academic Press.

Wainwright, P. C., Bellwood, D. R., Westneat, M. W., Grubich, J. R. and Hoey, A. S. (2004). A functional morphospace for the skull of labrid fishes: patterns of diversity in a complex biomechanical system. *Biol. J. Linn. Soc*. **82**, 1-25.

Wainwright, P. C., Ferry-Graham, L. A., Waltzek, T. B., Carroll, A. M., Hulsey, C. D. and Grubich, J. R. (2001). Evaluating the use of ram and suction during prey capture by cichlid fishes. *J. Exp. Biol*. **204**, 3039-3051.

Wainwright, P. C. and Shaw, S. S. (1999). Morphological basis of kinematic diversity in feeding sunfishes. *J. Exp. Biol.* **202**, 3101-3110.

Waltzek, T. B. and Wainwright, P. C. (2003). Functional morphology of extreme jaw protrusion in neotropical cichlids. *J. Morphol.* **257**, 96-106.

Westneat, M. W. (1990). Feeding mechanics of teleost fishes (Labridae, Perciformes): a test of four-bar linkage models. *J. Morphol*. **205**, 269-296.

Westneat, M. W. and Wainwright, P. C. (1989). Feeding mechanism of *Epibulus insidiator* (Labridae, Teleostei): evolution of a novel functional system. *J. Morphol*. **202**, 129-150.

Winterbottom, R. (1974). A descriptive synonymy of the striated muscles of the Teleostei. *Proc. Acad. Nat. Sci. Phil*. **125**, 225-317.

Wylie, C. R. and Paul, V. J. (1989). Chemical defences in three species of *sinularia* (Coelenterata, Alcyonacea). Effects against generalist predators and the butterflyfish *Chaetodon unimaculatus* Bloch. *J. Exp. Mar. Biol. Ecol.* **12**, 141-160.